Solid Freeform Fabrication 2022: Proceedings of the 33rd Annual International Solid Freeform Fabrication Symposium – An Additive Manufacturing Conference
Reviewed Paper

Strength Comparison of Topology Optimized Lattice From Printed SLA Resin, Electroplated Resin and PBF Aluminum Alloy

Sean Wise[1], Lourdes Bobbio[2], Analisa Russo[3], Timothy Simpson[4], Allison M. Beese[2]

[1]Repliform, Inc.; [2]Pennsylvania State University College of Earth and Mineral Sciences; [3]Formlabs Inc.; [4]Pennsylvania State University College of Engineering.

Abstract

Given the high cost of metal components made with powder bed fusion (PBF), we compare the strength of two electroplated resin components against monolithic stereolithography (SLA) polymer and BPF aluminum alloy copies of the same geometry. Using Rule of Mixtures (ROM) analysis, validated by ASTM tensile strength measurements, two coating sequences were designed to provide electroplated samples with half the tensile strength and approximately equal tensile strength to PBF AlSi10Mg, respectively. All four sets were subjected to 3-point bending. The monolithic materials had higher proportionate maximum load with respect to tensile strength; however, the electroplated polymer parts displayed enhanced bending response relative to their designed tensile strength. The plated resin part with weaker coating bore 85% of the load of the PBF AlSi10Mg part while the parts with a stronger coating bore almost twice the load of the PBF AlSi10Mg part in a 3-point bend configuration. The enhanced performance may be due to the surface reinforcement from the high strength coating, which better resists bending and buckling in this type of design.

Keywords: Structural Electroplating, Metal-Clad Composites, Electroplated AM Plastic, Topology Optimized Design

1. Introduction

High quality electroplated metal coatings add new function to stereolithography (SLA) 3D printed parts. With a structural metal skin and a lightweight resin core, these metal clad composites exhibit high flexural strength [1]. Metal coatings impart other metal-like qualities to 3D printed models including electrical conductivity [2,3], cosmetic finishes, and wear resistance. In addition, metal cladding protects SLA parts from environmental wear, particularly in applications requiring UV light exposure, high humidity, or even high vacuum. Electroplated 3D printed plastics find applications in the automotive and defense industries, manufacturing fixtures, and consumer product production.

Electroplating is an electrochemical process used to deposit thin layers of solid metal onto a surface via reduction of cations in solution [4]. The target substrate for plating must be electrically conductive, so pre-coatings have been developed which produce an ultra-thin conductive interface, allowing a variety of metals - most notably copper and nickel alloys - to be plated onto plastic parts [5,6]. Electroplated coating thicknesses range from 25 to 400 microns, depending on the application. Thinner coatings can be used for cosmetic and electrically conductive surfaces, while thicker coatings are required for structural reinforcement.

Mechanically reinforced parts studied in this paper are made from Clear Resin, provided by Formlabs Inc [7], clad with sequential electroplated layers of copper, ductile nickel, and hard nickel by Repliform Inc. The plating conditions that result in differing properties between ductile and hard nickel coatings are described in Section 2.1. With a 420 micron nickel-rich coating applied, we observed a 16x increase in tensile modulus and 30x increase in flexural modulus compared to as-printed Clear Resin. The ultimate tensile and flexural strength of SLA resin parts also exhibited significant improvement with the addition of metal cladding.

3D Printing can be leveraged to produce complex geometries not achievable through traditional molding or machining, and data-drive design methods such as topology optimization (TopOp) have emerged to take advantage of freeform fabrication [8]. TopOp computationally subtracts material from a model to minimize the volume required to achieve specific design constraints. The result is often a complex organic shape with high surface area to volume ratio. High surface area TopOp structures are a natural fit for electroplating because relatively thin coatings significantly increase the metal volume fraction of a resin part, efficiently enhancing its mechanical properties.

In this study a beam with organic truss-like geometry was designed using nTopology software and tested under 3-point bending. Using a predictive model based on rule of mixtures (ROM) analysis, two coating sequences were designed for Clear Resin to provide electroplated samples with half the tensile strength and approximately equal tensile strength to PBF AlSi10Mg [9], respectively. Under 3-point bending, the plated beam with weaker coating bore 85% of the load of an identical PBF Al alloy beam while the plated beam with a stronger coating bore almost twice the load of the PBF Al alloy beam. Data suggest that lightweight and low-cost structures generated via TopOp and metal clad SLA resins hold promise for mechanically demanding applications.

2. Background Research

Tensile (ASTM D638-14) and flexural (ASTM D790-15) mechanical properties of Formlabs Clear Resin sample bars clad with electroplated coatings of copper, ductile nickel, and hard nickel in various thicknesses were tested. These samples closely resemble electroplated thin-walled parts with plastic thickness ranging from 2.4 to 3.2 mm and metal coatings ranging from 38 to 420 microns thick. The results demonstrate a significant improvement in tensile modulus and ultimate tensile strength and a dramatic increase in flexural modulus and ultimate flexural strength compared to a control sample of as-printed Clear Resin.

2.1 Mechanical Properties of Electroplated Metal Films

Properties of metal coatings were obtained from a previous study that employed microtensile testing, developed specifically to probe local mechanical properties of laminates [10-14]. Specimens with gauge dimensions of 3 x 1 mm and ~0.30 mm were prepared from laminate areas of interest. Samples were tested using a benchtop micro load cell, and full stress-strain profiles produced.

The values shown in Table 1 correspond to properties of three electrodeposited metals: structural copper, ductile nickel, and hard nickel obtained from Nimer, et al. [10-11]. Hard nickel coatings have a grain size approximately 1/10 that of ductile nickel, with residual sulfur incorporated. This difference in microstructure and chemical composition is the result of differing plating conditions. In the case of hard nickel deposition, nickel sulfamate baths are run with insoluble anodes, and there is a byproduct reaction with the sulfamate ion that creates a compound in the bath resulting in a smaller nickel grain size with sulfur incorporated. Micrographs of ductile and hard nickel coatings indicating differences in grain size are shown in Supplemental Figure 1.

The metal cladding compositions studied in this paper are sequentially layered laminates composed of 2-3 metal coatings. The "Ductile" coating is composed of three equal thickness layers of structural copper, ductile nickel, and hard nickel. The "Hard" coating is a 90% nickel-rich coating composed of 42 microns of copper and 378 microns of hard nickel. Laminate properties are calculated from a weighted average of the constituent metal properties.

Metal Coating	Composition	Ultimate Tensile Strength (MPa)	Yield Strength (MPa)	Tensile Modulus (GPa)
Cu (Structural)	Cu	370	264	90
Ni (Ductile)	Coarse grain Ni	860	650	140
Ni (Hard)	Fine grain Ni	1558	1288	146
"Ductile" Coating	Equal layers Cu, Ductile Ni, Hard Ni	929	734	125
"Hard" Coating	10% Cu 90% Hard Ni	1439	1185	140

Table 1: Mechanical properties of electroplated metal cladding.

2.2 ASTM Tensile and Flexural Sample Preparation and Testing

2.2.1 Test Strip Design and 3D Printing

We prepared a complete set of ASTM tensile (D638-14) and flex (D790-15) sample bars in Formlabs Clear Resin to accommodate metal coating thicknesses of 38, 76, 152, 304, and 420 microns, plus an unplated control sample. Prior to printing, we modified the CAD files for the standardized test bars to offset external surfaces to accommodate the coating. As a result, all plated samples plus the unplated control had the same external dimensions. This design modification is outlined in Table 2.

Test strips were printed on a Formlabs Form 3 SLA printer at a 45 degree print orientation, with a layer height of 100 microns. The parts were thoroughly washed in IPA, completely dried, and UV cured using the recommended time and temperature settings. Support marks were carefully sanded off the supported edge.

For four of these samples (38, 76, 152, 304 μm coating thicknesses) Repliform employed the “Ductile” plating sequence outlined in Table 1: sequential equal layers of copper, ductile nickel, and hard nickel. The 90% nickel-rich “Hard” plating sequence was prepared for the 420 micron sample with 42 microns of copper and 378 microns of hard nickel (Table 1). Each bar was designed to achieve a specific metal volume fraction, however each physical bar was also weighed before and after plating, and the actual (measured) metal volume fraction was calculated. These values are shown in Table 2.

Resin Bar Thickness (cm)	Resin Bar Width (cm)	Coating Thickness (μm)	Coating Type	Nominal Metal Vol Fraction	Measured Metal Vol Fraction
3.2	12.72	0	No coating / as printed	0	0
3.12	12.64	38	“Ductile”	0.03	0.026 Tensile 0.028 Flex
3.05	12.57	76	“Ductile”	0.06	0.057 Tensile 0.057 Flex
2.9	12.42	152	“Ductile”	0.12	0.106 Tensile 0.106 Flex
2.59	12.11	304	“Ductile”	0.23	0.213 Tensile 0.204 Flex
2.36	11.88	420	“Hard”	0.31	0.314 Tensile 0.308 Flex

Table 2: Design modification of ASTM tensile and flex bars to accommodate “Ductile” and “Hard” electroplated metal cladding of various thickness.

2.2.2 Test Strip Electroplating

The plating process used is similar to the generic production processes developed for plating on plastics (ASTM B604-91) but the actual Cu & Ni electroplating baths follow ASTM B832-93 Standard Guide for Electroforming with Copper and Nickel, modified for structural applications [15-17]. This general process is outlined in the flow chart in Figure 1, however some intermediate steps are needed to ensure good adhesion between the resin and metal cladding.

It is important to begin with clean, well cured parts that have no uncured resin or foreign material contaminating the surfaces [18]. The parts are mounted to a rack with copper wires that are inserted through holes bored through thick ends of the geometry. The surfaces are etched by spraying them with a fine abrasive in all directions to give a uniformly dull appearance. Application of a conductive seed layer is done in a room temperature electroless nickel line in four steps that are each followed by a DI water rinse. This begins with soaking in soap solution to remove residual soils, then placed into a mixed activator-catalyst soak, followed by an accelerator tank that removes activator residues, and finished in a commercial room temperature electroless nickel bath that deposits 1 micron of electroless conductive nickel. Every step in this process is done at less than 38°C.

Parts are inspected to ensure complete conductive layer coverage and to ensure there is a good electrical connection to the rack. The electrolytic copper is deposited from an acid copper bath with a PEG type surfactant for grain refinement at a rate of 6 amps/foot^2 and then rinsed in DI water. The parts are then placed into a ductile nickel bath with 6 amps/foot^2 and then transferred to a hard nickel bath without rinsing. The appropriate thickness of deposited metal applied is based on total current Amp-hours/foot^2 in each bath.

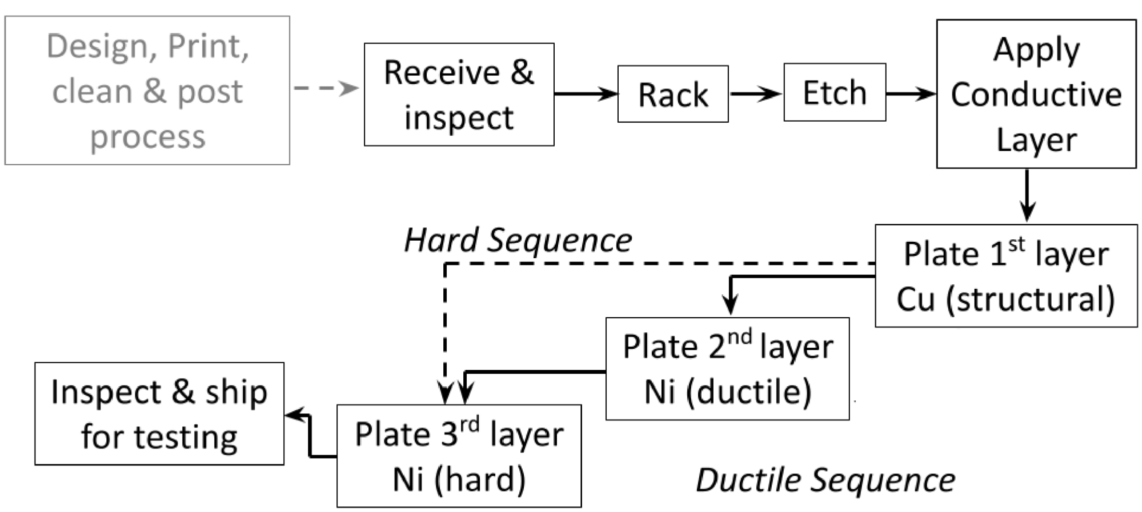

Figure 1: General plating process. There are numerous variations that can be made to each step to achieve coatings for cosmetic, electrical, or structural applications.

2.2.3 Test Strip Validation

All coatings are validated by weighing parts prior to racking and plating, and then weighing again after removal from the plating rack. Volume fraction of metal is calculated and compared to the original design plan using Equation 1, where f is the volume fraction of metal, m is mass, ρ is density, and subscripts m and p denote metal and plastic, respectively. The volume fraction of metal can be calculated directly by considering the local cross sectional area of the 3D printed resin bar in the active test area, and the thickness of the electroplated coating. However, due to slight variations in the thickness of the metal coating, a more accurate measurement of volume fraction is derived from this mass measurement, particularly with thin electroplated layers. From this point, we will refer to specific physical samples by their coating thickness, but analyze and predict laminate properties based on metal volume fraction.

$$f = \frac{m_m / \rho_m}{(m_m / \rho_m) + (m_p / \rho_p)} \qquad \text{Equation 1}$$

2.2.4 ASTM Tensile and Flexural Testing

Five copies of each sample type were tested using the methods outlined in ASTM standards D638-14 and D790-15. From stress-strain plots, tensile modulus, flexural modulus, ultimate tensile strength, and ultimate flexural strength were derived.

2.3 ASTM Tensile and Flexural Test Results

Typical molded solid walled part designs will have a wall thickness of 2-3 mm and typical metal coatings resulting in 6-15 vol% metal, so the test strips themselves are an accurate mimic of a thin walled plated part. At the higher end of the range we tested (above 25 vol% metal) these types of metal volume fractions are associated with very fine structural features like lattices, or objects that are designed with topology optimization.

First tensile and flexural modulus were plotted against volume fraction of metal, as outlined in Figure 2. The “Ductile” metal coating applied in thicknesses of 38, 76, 152 and 304 µm resulted in a nearly linear increase in all properties measured, compared to metal volume fraction. We observed over a 9x increase in tensile modulus and 18x increase in flexural modulus. A more dramatic effect was seen in the stronger “Hard” metal coating applied in a thickness of 420 microns. Here we observed a 16x increase in tensile modulus and a 30x increase in flexural modulus compared to as-printed Clear Resin.

Each sample was deformed until failure, and we quantified the ultimate tensile and flexural strength compared to volume fraction of metal. A similar linear pattern emerges in this data and we again see that metal plating has an amplified impact on flexural properties. The “Ductile” coating applied at a thickness of 304 microns resulted in a 3x increase in both tensile and flexural strength. The “Hard” coating applied in a thickness of 420 microns resulted in a 6x increase in tensile strength and nearly a 8x increase in flexural strength compared to as-printed Clear Resin. All results are outlined in Table 3.

Electroplating with copper and nickel shifts the properties of SLA 3D printed parts into a range that is sparsely occupied by additive manufacturing (AM) materials. Figure 2c places this data into the context of SLA, selective laser sintering (SLS) and fused deposition modeling (FDM) 3D printing materials at the low end of tensile modulus and strength, and common AM metals at the high end. The metal clad composites represented in light blue include Clear Resin as well as Formlabs Tough 2000 and glass-filled Rigid 10K Resins coated by the “Ductile” electroplating sequence. Our data for metal clad resin fills a wide gap, mimicking the tensile properties of fiber reinforced plastics such as 30% glass-fiber polyester.

The amplified effect of metal cladding on flexural properties may be due to the concentration of metal at the outer surfaces of the laminated composite which experience the highest tensile and compressive forces during bending. The metal coating has a disproportionate role in taking on the highest loads during bending, compared to the resin core. Images of metal-clad composite specimens before and after loading are shown in Supplemental Figure 2.

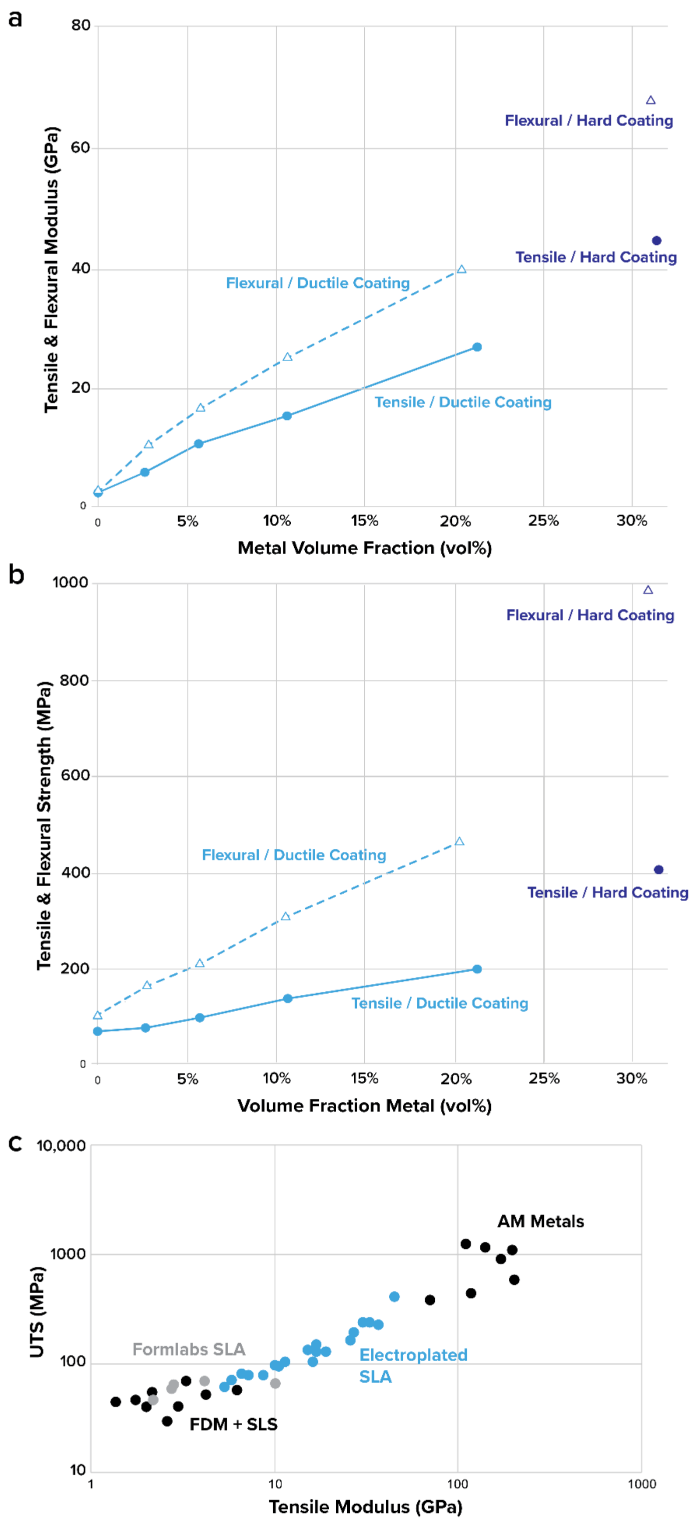

Figure 2: a) Volume fraction metal vs. tensile and flexural modulus of metal clad composites;
b) Volume fraction metal vs. ultimate tensile and flexural strength; c) UTS and tensile modulus of metal clad composites compared to common AM materials.

Coating Composition (metal thickness and type)	**Tensile Modulus (GPa)**	**Tensile Strength (MPa)**	**Flexural Modulus (GPa)**	**Flexural Strength (MPa)**
0.00 / As printed [7]	2.8	65	2.2	97
38 µm / “Ductile”	5.8 ± 0.68	70.3 ± 4.0	9.9 ± 0.37	161.3 ± 6.2
76 µm / “Ductile”	10.5 ± 0.50	94.4 ± 9.6	16.1 ± 0.47	208.2 ± 4.3
152 µm / “Ductile”	15.4 ± 1.5	133.7 ± 11	24.6 ± 1.4	304.7 ± 9.6
304 µm / “Ductile”	26.9 ± 0.68	196.5 ± 8.2	39.6 ± 1.5	461.2 ± 31.7
420 µm / “Hard”	44.9 ± 3.6	404.7 ± 7.6	66.8 ± 2.8	985.9 ± 20

Table 3: Tensile and flexural mechanical properties of metal clad composites composed of Clear Resin and copper-nickel coatings of various thickness.

2.4 Rule of Mixtures Prediction of Tensile Properties of Electroplated SLA Parts

A plated resin part is a metal-clad laminated composite in which the resin core and metal skin each contribute to the composite strength, stiffness, and weight of the part. Here both copper and nickel are used to produce a strong yet ductile coating.

We can predict the tensile strength and modulus of metal clad composites by employing a general rule of mixtures (ROM) analysis [19]. This predictive model hinges on a simple equation that takes a weighted average of the metal skin and polymer substrate properties. In Equation 2, E_c is the composite property (tensile modulus or strength), f is the volume fraction of metal, E_m is the metal coating property, and E_p is the plastic substrate property.

$$E_c = fE_m + (1 - f)E_p \qquad \text{Equation 2}$$

Using the metal properties reported in section 2.1 we generated an ROM model for Clear Resin clad with both the “Ductile” and “Hard” electroplating compositions, and overlaid this with plots of tensile modulus vs volume fraction metal for each composite sample. As shown in Figure 3, the model matches extremely well in both cases. Upon further examination, the slopes of the prediction lines are 137 and 122 GPa. These values should approximately match the moduli of the “Hard” and “Ductile” metal coatings, and in fact they do; these modulus values are 136 and 113 GPa, respectively.

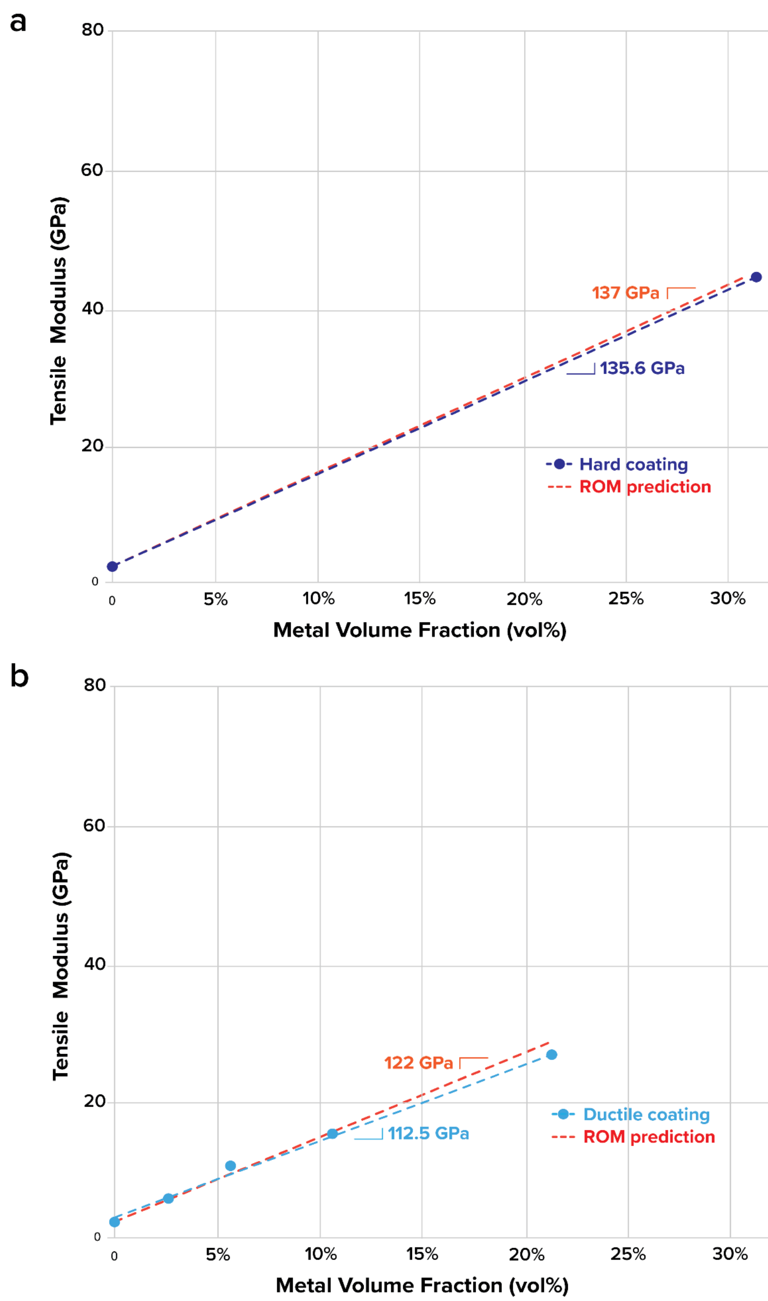

Figure 3: ROM predictions for tensile modulus of metal clad Clear Resin laminates with a) "Hard" and b) "Ductile" electroplated coatings. Predictions match well to experimental data.

3. Methods: Design and Loading of TopOp Structure

Background research presented in Section 2 demonstrates that composites of 3D printed resins and electroplated metal coatings with 3-25 vol% metal composition result in significantly enhanced tensile and flexural properties, compared to as-printed resins. The high surface area of

TopOp structures are a natural fit for electroplating because relatively thin coatings significantly increase the metal volume fraction of a resin part, leading to composites with high metal volume fraction.

In this study, we directly compared metal clad resin TopOp structures to a powder bed fusion (PBF) AlSi10Mg directly printed part of equivalent geometry. We found that upon failure, a plated part with 150 µm "Ductile" nickel coating bore 85% of the load of an identical PBF Al alloy part while a part with 250 µm "Hard" nickel coating bore almost twice the load of the PBF Al alloy part.

3.1 Design of the TopOp Beam

A trussed beam structure was selected from the nTopology design library that was suited for the 3-point bend hardware. Outer dimensions are 62 x 15 x 10 mm, as shown in Figure 4.

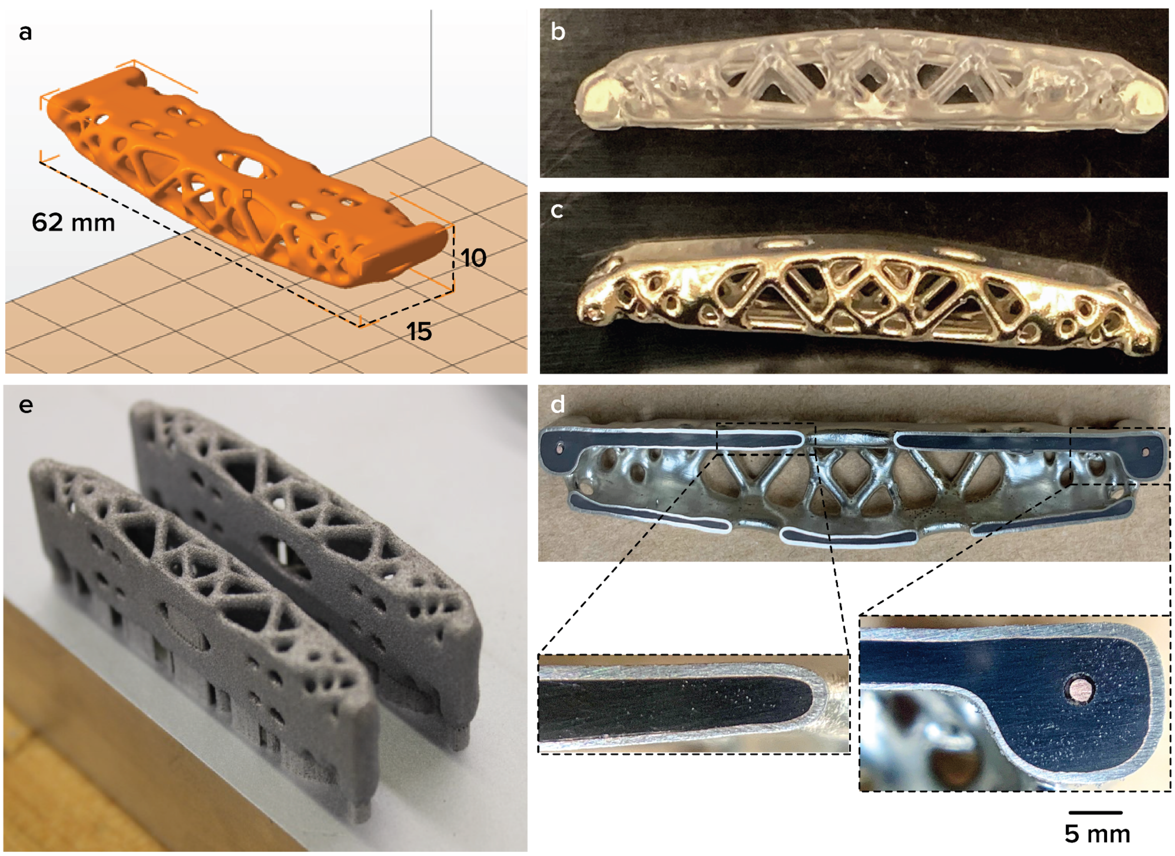

Figure 4: a) TopOp beam design in nTopology software; b) TopOp beam as-printed in Formlabs SLA Clear Resin; c) TopOp beam printed in Clear Resin, surface offset by 150 µm, and clad with 150 µm "Ductile" electroplated coating; d) Cross section of Clear Resin TopOp beam clad with 250 µm "hard" Ni coating; e) TopOp beam printed in PBF AlSi10Mg sintered powder.

3.2 Preparation of TopOp Beams

3.2.1 Clear Resin Beam

A control sample was printed without modifications in Formlabs Clear Resin on the Form 3 stereolithography 3D printer. The part was thoroughly washed in IPA, dried, and cured using the recommended time and temperature settings.

3.2.2 *Metal clad Composite Beams*

Two plating sequences were developed for Clear Resin structures to match half and approximately equal tensile strength of PBF AlSi10Mg (annealed) [9]. The plating sequences used for the weaker and stronger TopOp bars matched the "Ductile" and "Hard" coatings described and tested in Section 2, respectively.

ROM analysis was applied to the entire TopOp structure using the tensile modulus of the "Ductile" and "Hard" coatings (Table 1), the modulus of Formlabs Clear Resin (Table 3), and our goals for laminate tensile strength. We determined that 150 microns of the "Ductile" coating would achieve our goal of approximately 50% tensile strength of PBF AlSi10Mg, on average over the entire TopOp structure. Likewise, 250 microns of the "Hard" coating would result in slightly higher tensile strength compared to PBF AlSi10Mg over the entire structure.

The design files for the TopOp beams were modified to incorporate appropriate surface offsets so the envelope geometry of every sample was identical. The files were also modified to include mounting features for placement in the electroplating bath. These features were added to the tips of the beam, in areas that are not critical to the function of the beam during a 3-point bending configuration. Images of a plated TopOp beam are shown in Figure 4.

3.2.3 Sintered Aluminum Alloy (PBF AlSi10Mg) Beam

Finally a TopOp beam sample was produced using EOS Aluminum AlSi10Mg alloy powder and an EOS M 290 printer. The printed beam was subjected to a stress relief heat treatment at 270 °C for 1.5 hours. The material properties reported by EOS are listed in Table 4.

3.3 Loading of TopOp Beams

All samples were subjected to 3-point bend test using an MTS 642.001 Bend Fixture, with a roller span of 50 mm as shown in Figure 5. A crosshead loading speed of 0.6 mm/min was used, and the force versus displacement signals were collected. Each test was performed 2-6 times.

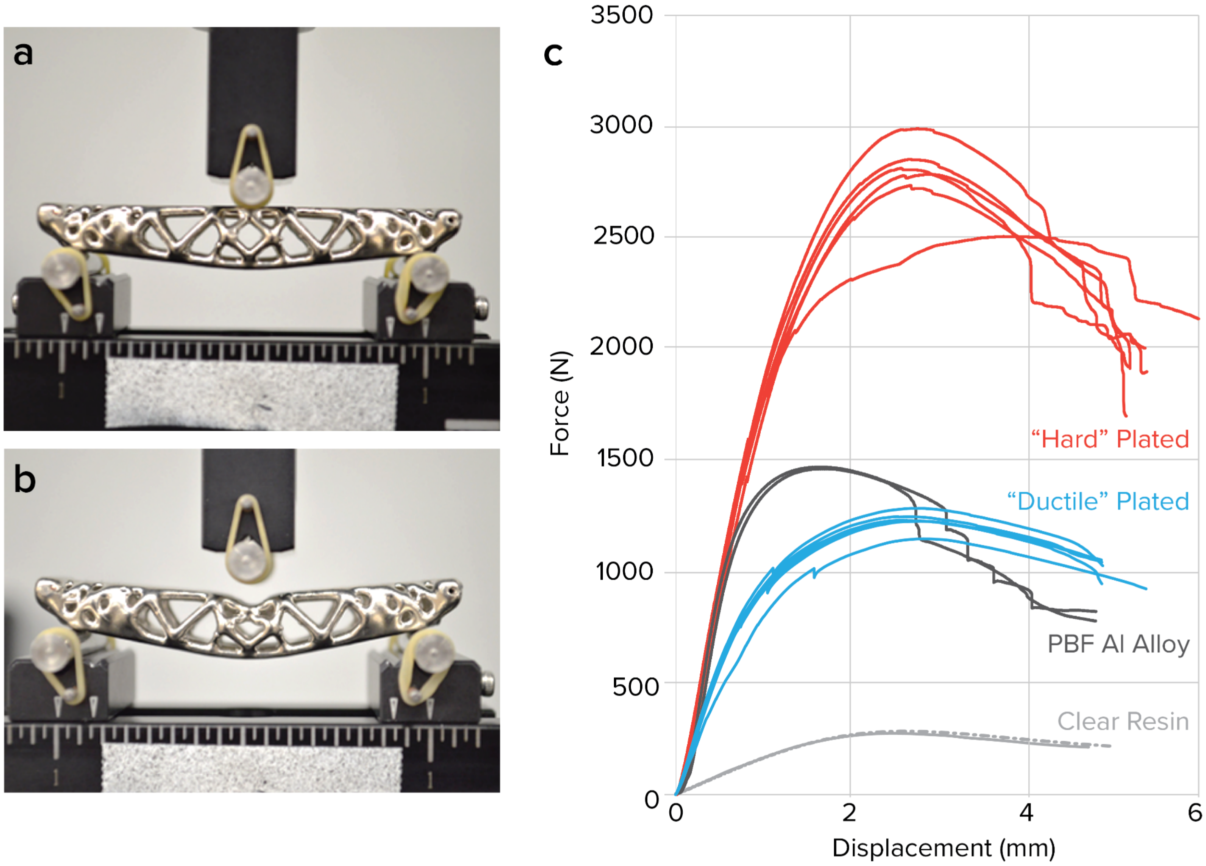

Figure 5: a-b) Experimental test setup of 3-point bend test on TopOp sample printed in Clear Resin and clad with 250 µm “Hard” electroplated coating, before and after loading; c) Force versus displacement behavior of TopOp samples, fabricated with four different methods, subjected to 3-point bending.

4. Results and Discussion: TopOp Structure

4.1 Deflection and Deformation of TopOp Beams

Force-displacement curves for each TopOp sample type (Clear Resin control, “Ductile” plated, “Hard” plated, and PBF AlSi10Mg), are shown in Figure 5. The initial elastic slope (N/mm) and maximum force for each sample are given in Table 4. The metal clad resin with “Hard” electroplated coating outperformed PBF AlSi10Mg part with regard to maximum applied load at failure. In fact, it can withstand nearly double the applied force.

Specimen	Composition	Tensile Modulus (GPa)	UTS (MPa)	Maximum Load (N)	Loading Slope (N/mm)
Clear Resin [7]	Not plated	2.8	65	279.7	169.7
"Ductile" Plated SLA **21 vol%**	Clear Resin **150 µm "Ductile" Coating**	26.9	196	1244	1055
"Hard" Plated SLA **34 vol%**	Clear Resin **250 µm "Hard" Coating**	44.8	404	2829	2025
PBF AlSi10Mg [9]	Sintered Aluminum **(annealed)**	70	320	1460	1912

Table 4: Tensile Modulus and Ultimate Tensile Strength (UTS) of Clear Resin and PBF AlSi10Mg are obtained from datasheets. Tensile Modulus and UTS of plated parts are calculated from ROM analysis of the entire structure. Maximum Load and Loading Slope are obtained from the 3-point bend test results.

4.2 Mechanics of TopOp Beam Failure

The laminated nature of the metal clad composites can again help explain why they perform well in a bending configuration. Here local trusses in the TopOp samples fail in bending and buckling, which are flexural motions. The surface of the electroplated part, where the metal component is concentrated, is taking on the maximum load during part deformation.

Generally the electroplating process builds up a greater thickness of metal on positive features compared to recessed features, due to the line-of-sight nature of the plating process. This is particularly apparent in the TopOp beam that we studied, as shown in the cross section image in Figure 4. Note that distribution of metal coating works to our advantage when it comes to mechanical reinforcement; the highest build up is on the external surfaces, where it has the greatest contribution to bearing a flexural load.

4.3 Material cost

A part cost analysis was performed based on typical prices of outsourcing SLA printing, PBF printing, and electroplating at various production scales. For the TopOp beam produced for this study, electroplated resins are quite competitive with PBF AlSi10Mg particularly in larger batch production (over 10 units). These findings are summarized in Table 5.

Price Per Part

Material	Qty 1	Qty 2	Qty 3	Qty 10	Qty 20	Qty 30
PBF AlSi10Mg	$251	$198	$180	$155	$150	$148.50
SLA Acura 60	$57	$46	$41	$30	$28	$27.70
150 µm "Ductile" Plating	-	-	-	$52	$27	$19
"Ductile" Plated Composite	-	-	-	$82	$55	$46.50
250 µm "Hard" Plating	-	-	-	$72	$37	$25
"Hard" Plated Composite	-	-	-	$102	$65	$52.7

Table 5: Cost per TopOp part, produced at various batch quantities. Plated composite values shown in black represent the sum of the corresponding SLA resin printing cost and plating cost.

5. Conclusions and Future Work

Structural electroplating and topology optimization are complementary methods that produce strong, stiff, and lightweight parts that are difficult to achieve by 3D printing alone.

Through this study, we found that ROM analysis provides an accurate predictive model for tensile properties of metal clad composites. However due to the concentration of metal cladding on the outer surfaces of the composite, electroplating has a significantly amplified impact on flexural properties. This effect is amplified even further by the line of sight nature of the electroplating bath, which deposits a thicker metal layer on outermost surfaces of a latticed or truss-like model. As a result, a TopOp design that fails in bending and buckling took on a higher load compared to an identical structure printed in PBF AlSi10Mg.

While high surface area of TopOp designs are clearly well suited for efficient mechanical reinforcement with electroplating, further study is required to develop predictive models for metal clad composites with complex geometry. Namely, parameters within TopOp design tools such as nTopology could be specifically developed to accommodate electroplated coatings, and truly take advantage of this hybrid manufacturing technique.

References

1. N. Saleh, N. Hopkinson, R.F.M. Hague and S. Wise, "Effects of Electroplating on the Mechanical Properties of Stereolithography and Laser Sintered Parts," *Rapid Prototyping Journal,* vol. 10, no. 5, 2004.
2. N. Lazarus, S.S. Bedair, S.H. Hawasli, M.J. Kim, B.J. Wiley and G.L. Smith, "Selective electroplating for 3D-printed electronics," *Adv Mater Technol.*, vol. 4 no. 8, 2019.
3. J.P. Le Sage, "3D Printed Waveguide Slot Array Antennas,'' *IEEE Access,* vol. 4, March 2016.
4. M. Schlesinger and M. Paunovic, *Modern Electroplating,* 5th ed. John Wiley & Sons Inc., Hoboken, NJ, USA, 2010
5. D. Li, K. Goodwin, C. Yang, "Electroless copper deposition on aluminum–seeded ABS plastics," *J Mater Sci.* vol. 43, 2008.
6. S.C. Domenech Jr, E. Lima, V. Drago, J.C. De Lima, N.G Borges, A.O.V Avila and V. Soldi, "Electroless plating of nickel–phosphorous on surface-modified poly(ethylene terephthalate) films." *Appl Surf Sci,* vol. 220, 2003.
7. Material Datasheet Standard, Formlabs Inc., 2017. [Online]. Available: https://formlabs-media.formlabs.com/datasheets/Clear_Resin_Technical.pdf
8. L. Jikai, et al., "Current and future trends in topology optimization for additive manufacturing," *Structural and Multidisciplinary Optimization,* vol. 57, 2018.
9. EOS Aluminium AlSi10Mg Material Data Sheet, EOS GbmH, 2022. [Online]. Available: https://www.eos.info/03_system-related-assets/material-related-contents/metal-materials-and-examples/metal-material-datasheet/aluminium/material_datasheet_eos_aluminium-alsi10mg_en_web.pdf
10. S. Nimer, J. Wolk and M. Zupan, "Local property characterization of friction stir welded Ti-5111: Transverse orientation measurements," *Acta materialia,* vol. 61, no. 8, 2013.
11. S Storck, J Esteeves, and M. Zupan, "Development of new lightweight hybrid sandwich cores using FDM technology" *SAMPE Journal,* vol. 48 no. 4, pp. 6-12, 2012.
12. M.E. Duffy, "Microtensile Characterization of Additively Manufactured AlSi10Mg," Ph.D. dissertation, Univ. Maryland, Baltimore, MD, USA, 2018.
13. C.L. Cheng, "Mechanical and microstructural characterization of copper microsamples after cold drawing," Ph.D. dissertation, Univ. Maryland, Baltimore, MD, USA, 2008.
14. D. Gianola and W. Sharpe Jr, "Techniques for testing thin films in tension," *Experimental Techniques,* vol. 28, no. 5, 2004.
15. Standard Guide for Electroforming with Copper and Nickel, ASTM B832-93, 2018.
16. Specification for Decorative Electroplated Coatings of Copper/Nickel/Chromium on Plastics, ASTM B604-91, 2019
17. *Tool and Manufacturing Engineers Handbook,* vol. 8 *Plastic Part Manufacturing*, Society of Manufacturing Engineers, Dearborn, MI, USA, 1996, Chapter 9: Coatings, Metal Deposition.

18. Preparation of Plastic Materials for Electroplating, ASTM B727, 2020.
19. S. Wise and R. Connelly, "Prototyping Thin-Walled Metal Parts via Electroforming over SL Models," *Rapid Prototyping and Manufacturing,* SME, 2004.
20. N.A. Fleck, V.S. Deshpande and M.F. Ashby, "Micro-architected materials: past, present, and future," *Proceedings of the Royal Society,* vol. 466, 2010.

Supplemental Figures

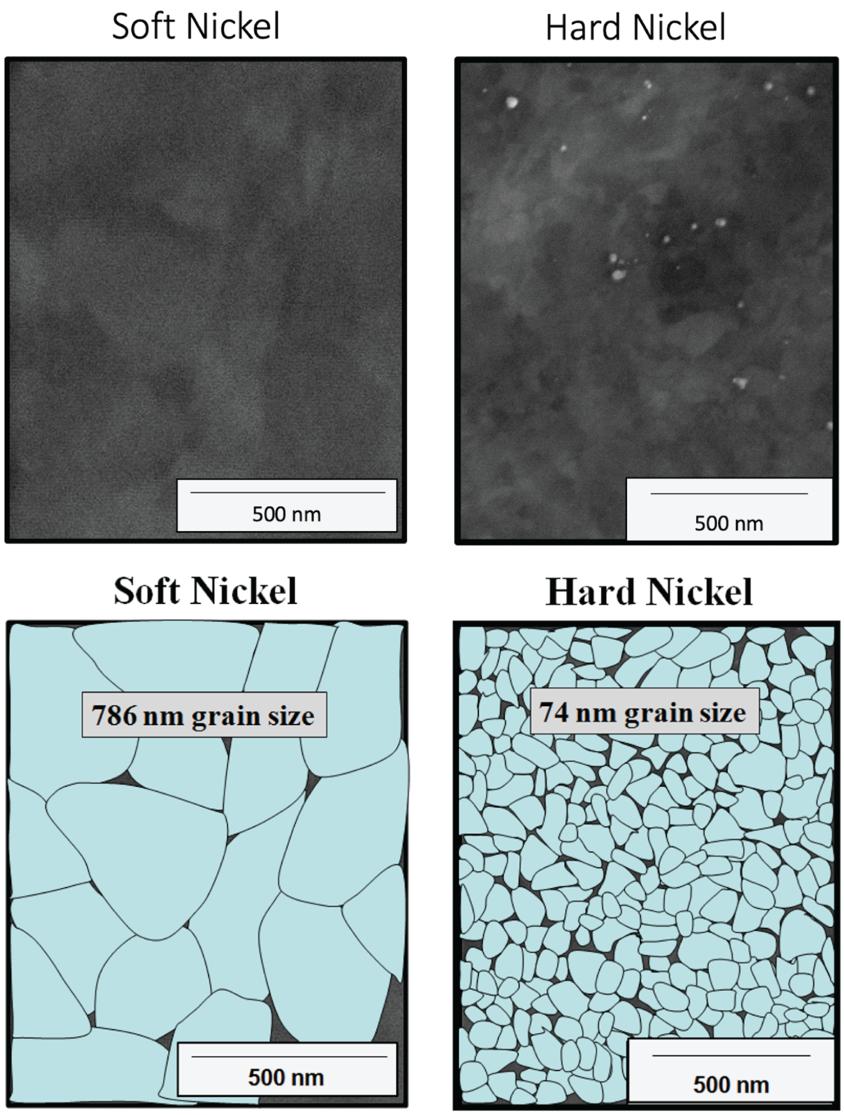

Supplemental Figure 1: Grain analysis of electrodeposited soft (ductile) and hard nickel coatings [20].

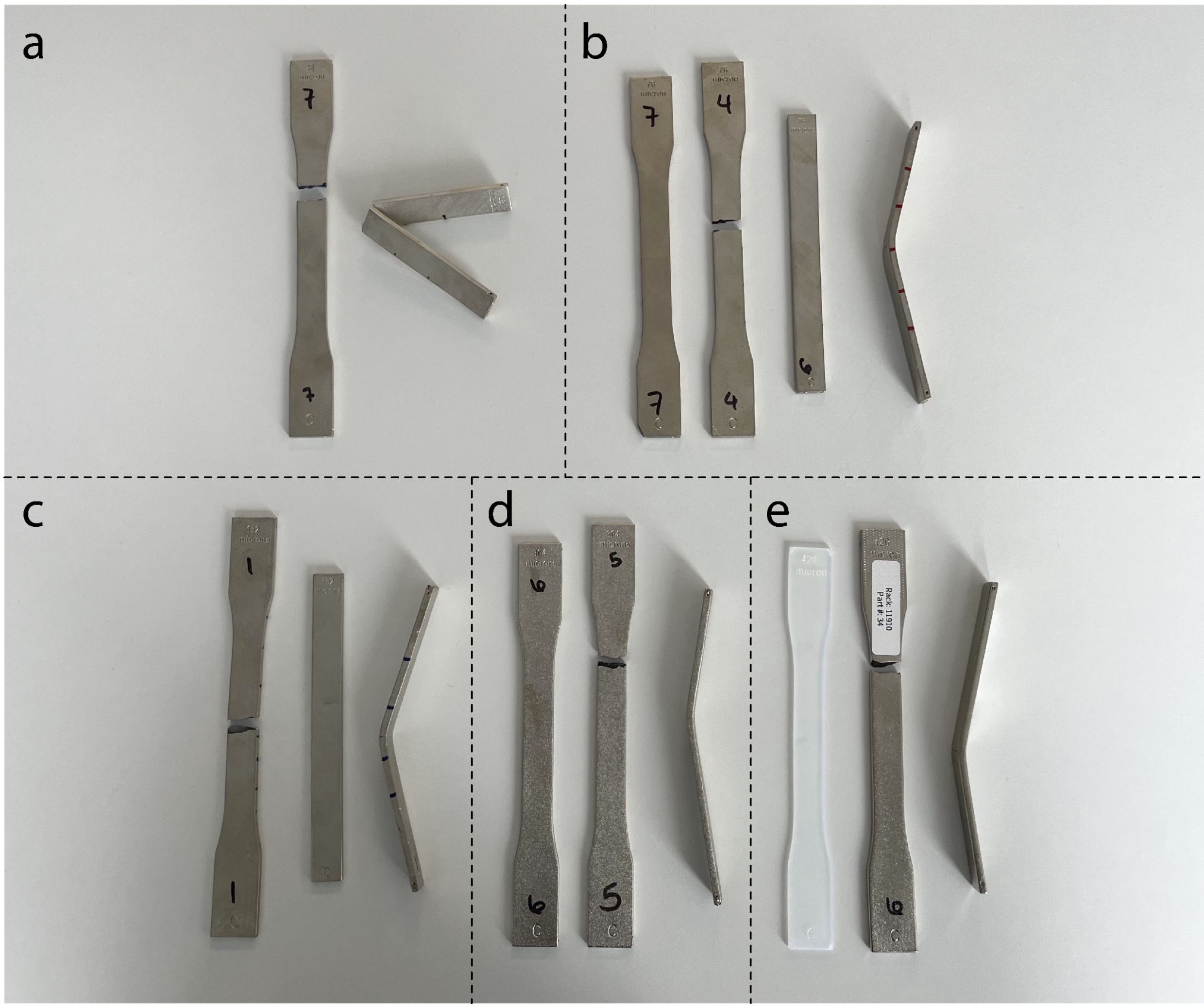

Supplemental Figure 2: Metal clad Clear Resin specimens before and after tests ASTM D638-14 (tensile) andASTM D790-15 (flexural). All in-tact samples are untested; bent or broken samples have undergone testing. a) 38 µm / “Ductile” b) 76 µm / “Ductile” c) 152 µm / “Ductile” d) 304 µm / “Ductile” e) 420 µm / “Hard.” An as-printed, unplated tensile bar is also shown.